Chapter 2

Translating Solid-Phase Conformational Memory in the Prophecy of Multi-stimuli Responsive Low Molecular Weight Gels

2.1 INTRODUCTION

Interest in low molecular weight gels is increasing rapidly in diverse fields, from pharmaceutical crystallization,[1-3] drug delivery, [4] optoelectronics, [5] catalysis [6] to environmental remedies [7]. Tuning self-assembly performance at molecular level is intuitive in designing a seemly gel for its potential applications [8]. The ability of these soft materials to translate molecular information to its nanostructured materials followed by the mesoscopic assemblies can severely impact on the physical properties of the dynamic resulting materials [9]. The evolution of a gel from a gelator molecule starts with self-assembling into an aggregate that lead to the formation of 1D supramolecular tapes into fibres. These 1D fibres are entangled to form a 3D solid-like network that immobilizes the solvents [10]. In many cases, gelators form gel in those solvents where they have an intermediate solubility and require some external triggers to solubilize or disperse them in the solution. Based on the solvent properties gelator's solubility varies and different outcomes of gel screening may appear: it may form gel, precipitate or crystals, and other structures. The role of solvents in gel formation is interpreted by considering solubility and thermodynamic parameters of solvent-gelator interactions. In both the cases where the gelator is highly soluble or insoluble they failed to form any gel. However, by changing the solubility of the gelator, it is highly possible to form a gel. Heating the solution is the easiest way to increase the solubility and also the most common approach to prepare a gel [11]. Other techniques such as solvent addition, and pH change are also frequently used to prepare gel by changing the gelator's solubility in the solvent. For example, hydrogelator 2NapFF that failed to form a gel by simple heating-cooling process, was abled to form a gel by three different ways: a) by addition of divalent salt; b) changing the pH from high to low and c) by adding anti-solvent (DMSO) to an aqueous solution of the gelator [12]. Different methods like Hansen solubility parameters (HSP), [13] Kamlet−Taft parameters, [14] Flory−Huggins parameter, [15], etc. were proposed to understand the role of a solvent in gel formation and to identify the nature of solvents that may form gel for the gelator under consideration. Diehn et.al used 1,3:2,4-di-benzylidene sorbitol (DBS) as a gelator to demonstrate correlations between the HSPs with the gelator's solubility at a particular temperature and concentration. They constructed 3D plots showing four different regions marked as solubility (S), slow gelation (SG), instant gelation (IG), and insolubility (I) for DBS in the different solvents. Based on the distance of the region from the center of the

3D plot they were able to predict the nature of the gel formed by DBS for a particular solvent [16].

Again, how the gelator is assembled in the solvent is greatly influenced by the nature of the solvent and ultimately decides the properties of the gel. Boc-D-alanine and Boc-L-alanine showed two different morphologies, macroporous honeycomb and aligned fibre bundles, in chloroform and toluene due to the difference in the self-assembly pathways of these molecules in the media [17]. The self-assembly process follows different favorable pathways (the pathway complexity) for fibre and/or network construction resulting in a self-regulating gel [18]. Nevertheless, there are challenges with reproducibility as emphasized by Draper and Adams [19]. The subtle experimental possessions in reproducing identical gel are critical. For example, the preparation method of gels is considered to be indispensable for varied morphologies and macroscopic properties. Most preparation methods involve the use of stimuli that trigger the formation of gel; i.e. heat-cool, sonication, [20-23] shaking, [24] light, [25] electric field, [26] addition of ions and change in pH or solvent polarity, etc [27-31]. The tris-urea gelator reported by Yamanaka et al. is a good example that responds to multiple stimuli, and a set of gels can be prepared just by varying the gelation procedure [13]. It is worth citing that the use of different types of stimuli such as addition of salt, and change in pH of the system can change in the rheological properties of the gels [12]. Reports identified three morphologically varied gels viz. hyperhelical (HH-Gel), tape-fibre (TF-Gel), or liquid crystalline (LC-Gels) from the same gelator by changing the method of preparation in the same solvent [32]. These assemblies are dynamic, and resulting gels are in kinetically trapped metastable state. The cholesteryl anthraquinone-2-carboxylate (CAQ) gel fibres are different from normal crystallization outcomes and identified as a new polymorph by Weiss et al [35]. Polymorphism in the azobenzene gel systems is based on the chromophore stacking and hydrogen bonding patterns showing varied thermodynamic stabilities and their formation kinetics [36]. It is driven by the solution-assembly pathway, solvent, temperature, and/or environmental parameters. Escuder and co-workers reported L-proline-based hydrogelator as a reusable heterogeneous catalyst for the direct aldol reaction [37]. They observed reproducibility issues when some samples failed to form hydrogels; instead, they formed weak gels, dispersions, or precipitate. On further investigation, they found that the gelator was polymorphic and identified four polymorphs of the material under different preparation conditions of the gel. The catalytic activity of the gelator's polymorphs for the direct aldol reaction between

cyclohexanone and 4-nitrobenzaldehyde was performed and a difference in the reaction rates was observed. They emphasized the role of temperature, aging time, ultrasound, and pH switching on the self-assembly course resulting in new phases with unlike gelling and catalytic properties [38].

The molecular solid state polymorphism is of great importance due to its impact on the physical properties like solubility, stability, morphology, etc. of the material concerned. Different polymorphic forms may show the difference in their properties that might be of importance in industries like pharmaceuticals. Polymorphic conversion during manufacturing, packaging, storage, and transportation may lead to poor therapeutic performances [39]. Thus, it became a legal requirement to provide the solid-state polymorphic behaviour of a drug along with the other documents seeking approval for commercialization from the state authorities. However, prior in developing a gel, this phase behaviour and intermolecular-relationship of the synthesized gelator have been obscure, despite being availability of ample studies on polymorphism highlighting its key role [40-44].

Considering polymorphism as the primary cause of solubility variation which plays a key role in determining gel performances, the role of polymorphism in low molecular weight gelator has been investigated. **G1** was designed with specific features to encourage self-assembly into fibers (structure of **G1** is shown in Scheme 2.1). Bis-urea functionality was incorporated because they strongly promote one-dimensional (1D) assembly, leading to the formation of gel fibers. Tetramethylxylylene spacer was used as the core structure for the gelator's design due to the bulky methyl groups on this spacer influence the molecule's shape and packing, favoring the formation of gel fibers. Di-acetal groups were used as endgroups for **G1** as these endgroups play a vital role in balancing the molecule's solubility and precipitation in the gelling solvent(s). Furthermore, the flexible bonds within the acetal groups allow for multiple molecular conformations, potentially leading to different polymorphic forms of the gelator. **G1** was synthesized and characterized using different analytical techniques to confirm the structure. Three different polymorphic phases were isolated by polymorph screening andthe gelling performance of each polymorph was examined. It was observed that the nucleation events and phase relationships on aggregation of thousands to millions of molecules is indeed a decisive factor of how the cascade of fibre branching propagates through opening up non-covalent interaction sites leading to dissimilar gel formation.

This study thus acquaints with a strategic impetus in tweaking the long-term stability of dispersion in the multi-stimuli responsive LMWG.

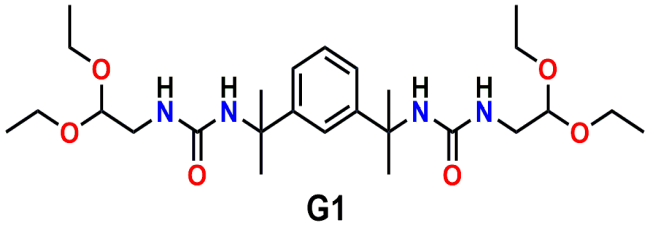

Scheme 2.1 Molecular structure of **G1**

2.2 RESULTS AND DISCUSSION:

2.2.1 Synthesis and Characterization of G1:

The bis-urea functionalized gelator **G1** (1,1'-(1,3-phenylenebis(propane-2,2-diyl))bis-(3-(2,2-diethoxyethyl)urea) was synthesized by following scheme 2.2, for synthesis of 1mmol equvalent of **G1** 2 mmol (0.27 g or 0.29 ml) of aminoacetaldehyde diethylacetal ($C_6H_{15}N_1O_2$) in 20 ml dry chloroform was added dropwise to the 30 ml of dry chloroform solution of 1 mmol (0.24 g or 0.23 ml) of 1,3-bis(2-isocyanatopropan-2-yl)benzene ($C_{14}H_{16}N_2O_2$) and kept stirring for 12 hour at room temperature (as shown in Scheme 2.2) . The reaction progress was monitored through thin layer chromatography (TLC). After completion of the reaction, the reaction mixture was evaporated to dryness under reduced pressure using rotary evaporator. Recovered crude product was washed with water and air dried to get **G1** as white powdery material, where the yield obtained was found to be 91% (0.46 g). The product was confirmed by different characterization techniques such thermal, spectroscopic, microscopic methods, and X-ray diffraction (Figure 2.1).

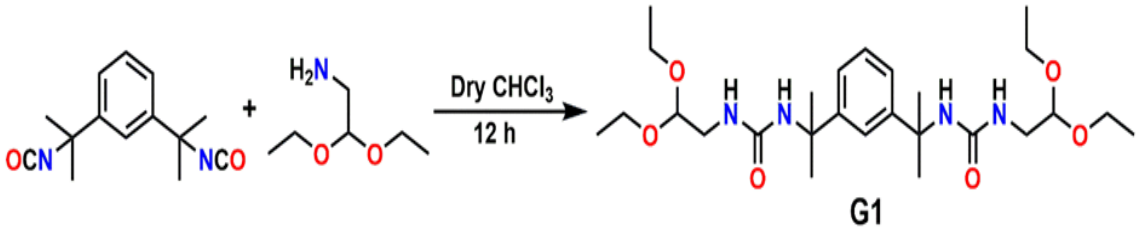

Scheme 2.2 Synthesis of a bis-urea low molecular weight gelator **G1**

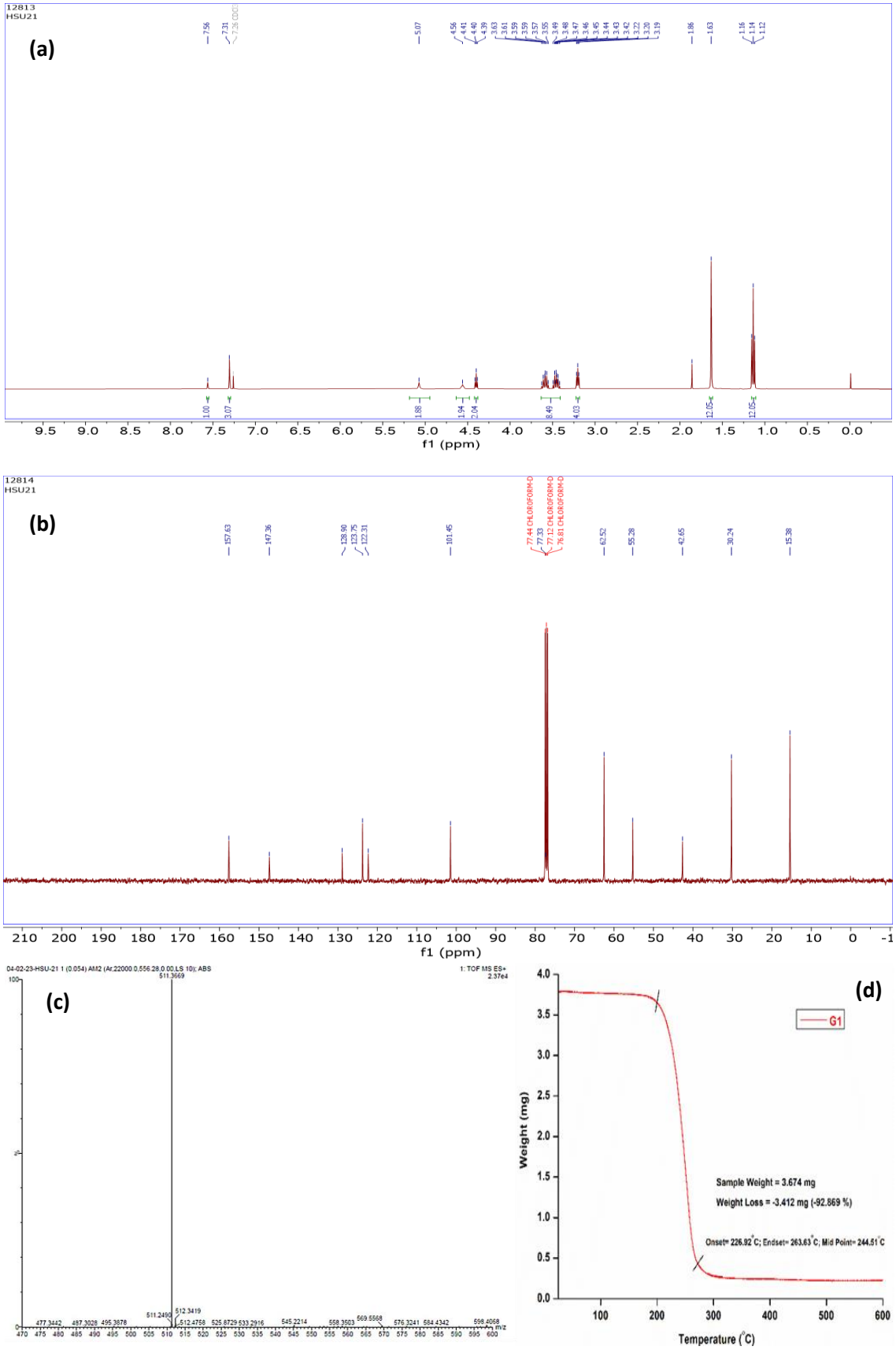

Figure 2.1 Different characterization results of **G1**: (a)^{1}H NMR spectra, (b)^{13}C NMR spectra, (c) HRMS, and (d) TGA thermogram

To know more about the structural insight of **G1**, solution crystallization experiments were carried out in different solvents to grow crystals but only DMF produced suitable crystals for single crystal X-ray diffractionanalysis (SCXRD).

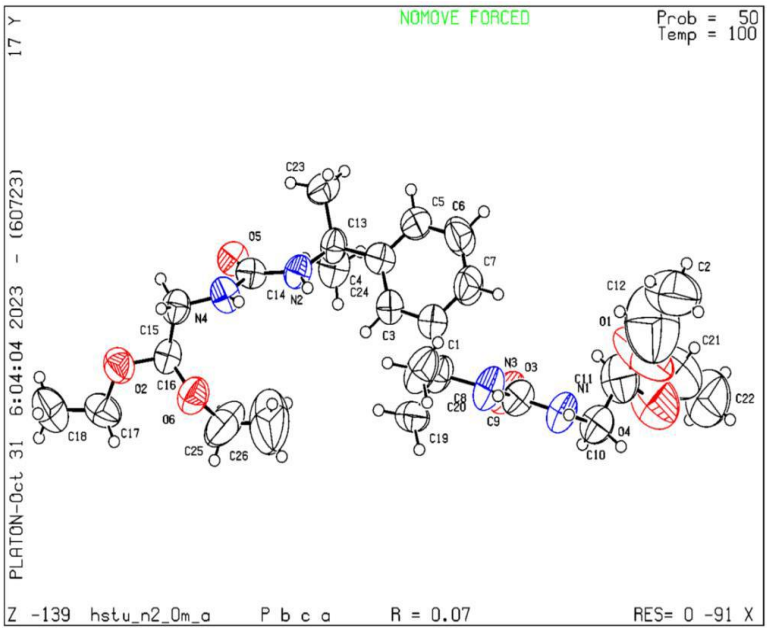

Figure 2.2 ORTEP diagram of **G1**

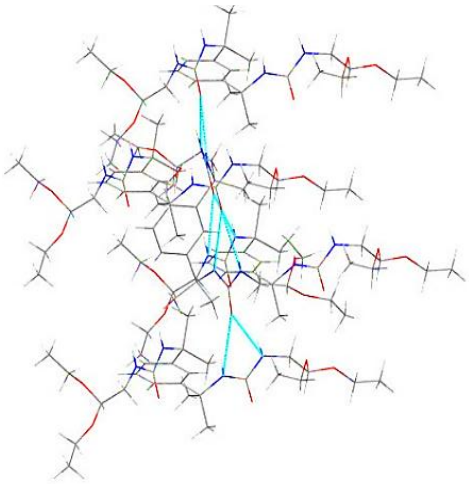

Figure 2.3 Intermolecular interactions in **G1** molecules in the crystal structure.

Single crystal XRD data of **G1**, structure was resolved in *Pbca* space group of the orthorhombic crystal system with one molecule in the asymmetric unit (ORTEP diagrame shown in Figure 2.3). Single-Crystal X-ray Diffraction Data Parameter of **G1** is tabulated in Table 2.1. Crystal growth of of **G1** is directed via bifurcated N–H···O hydrogen bonding between *bis-urea* moieties in a typical two-dimensional α-tape network extending through [010] axis (Figure 2.3). The weak C–H···π and C–H···O

interactions complete the three-dimensional packing of **G1** Form III crystals (H-bonding parameters are listed in Tables 2.2).

Table 2.1 Single-Crystal X-ray Diffraction Data Parameter of **G1**

Emp. Form.	**$C_{26}H_{46}N_4O_6$**
Form. Wt.	510.67
Cryst. Syst.	Orthorhombic
T [K]	100
a [Å]	14.5556(7)
b [Å]	9.2140(4)
c [Å]	44.491(2)
α [°]	90
β [°]	90
γ [°]	90
V [Å3]	5966.9(5)
Sp. Group	*Pbca*
Z	8
D_{calc} [gcm^{-3}]	1.137
μ (mm^{-1})	0.081
Uni. Refls.	4132
Obs. Refls.	1391
R1 [I >σ(I)]	0.0714
Wr2	0.2275
GOF	0.895
Instrument	Bruker D8Quest
X-ray	Mo Kα; λ = 0.71073
CCDC no.	2304758

Table 2.2 Inter H-bond and Intra H-bond parameters of **G1** in crystal structure

Inter H-bond

Interaction	H···A (Å)	D···A (Å)	∠D–H···A (°)	symmetry code
N_1–H_1···O_3	1.99	2.8036(1)	153	1/2-x,1/2+y,z
N_2–H_2···O_5	2.19	2.9972(1)	153	1/2-x,1/2+y,z
N3–H3···O_3	2.34	3.0484(1)	149	1/2-x,1/2+y,z
N4–H4···O_5	2.14	2.9561(1)	154	3/2-x,1/2+y,z

Intra H-bond

Interaction	H···A (Å)	D···A (Å)	∠D–H···A (°)	symmetry code
C_7–H_7···N_3	2.50	2.8416(1)	101	
C_{19}–H_{19C}···O_3	2.53	3.0720(1)	115	
C_{23}–H_{23C}···O_5	2.59	3.2032(2)	121	
C_{24}–H_{24B}···O_5	2.45	3.0345(1)	118	

The BFDH morphology prediction (Figure 2.4) further supported the crystal growth that occurs through its major nucleating plane(111). Multiple dangling hydrophobic moieties like –CH_2–, –CH_3, etc. on both sides of the central phenyl ring offers in propagating those weak interactions into a new non-covalent network structures accountable for gelation ability. The non-covalent interactions responsible for **G1** crystals were quantified by Hirshfeld Surface analysis (Figure 2.5). Apparently contribution of polar O···H interaction is higher (6.9%) than that of C···H (3.2%) and N···H (0.6%) interactions. The hydrophobic groups and weak non-covalent interactions essentially invite non-polar solvents to trap into the nooks spawned in **G1**, developing a gel.

(a) (b)

Figure 2.4 BFDH morphology analysis of crystal of **G1**

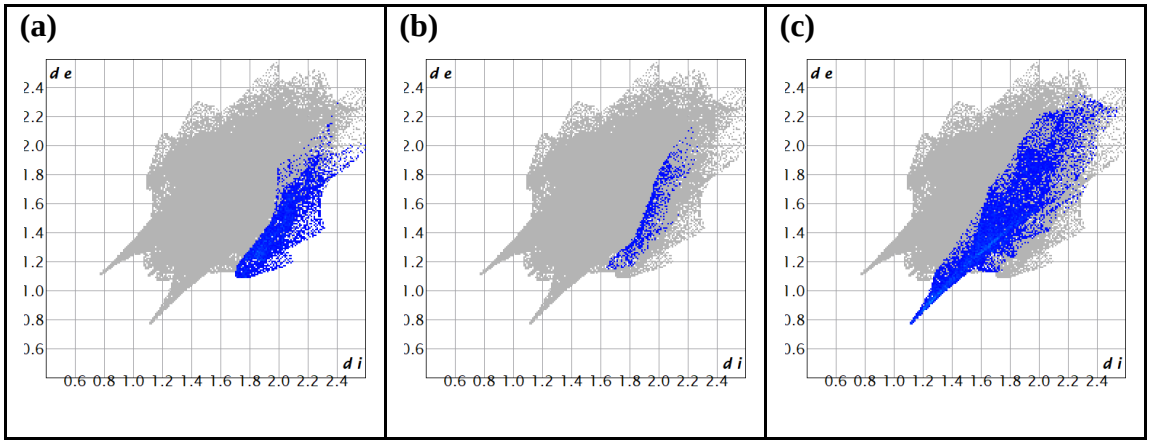

Figure 2.5 Hirshfeld surface analysis of crystal of **G1**; (a) C–H, (b) N–H and (c) O–H interactions

Although only one type of crystals grown in DMF but the occurrence of multiple solid phases of **G1** may be speculated from the presence of flexible end groups in **G1**. This flexible groups increases the probability to attain energetically related conformations concomitantly obtainable in the solution. Thus, the adjustment of conformation continuously occurs in the closely related conformations to minimize the lattice energy during crystallization events, leaving the possibility of finding more crystalline phases.

Density Functional Theory calculations at level basis set B3LYP/6-311G^{++} (d,p) was performed to treasure hunt possible energetically related conformations that could upshot dissimilar phases of **G1** [45]. Based on dihedral (or torsion) angles τ_1 & τ_2 (as shown in Figure 2.6), numerous conformations were found accessible for **G1** within a narrow energy window of approximately 10 kcal/mol and that too within the restrictions of only two dihedral angles quoted.

Therefore, there is high probability of the finding of multiple crystalline forms by thorough polymorph screening exercise with **G1**.

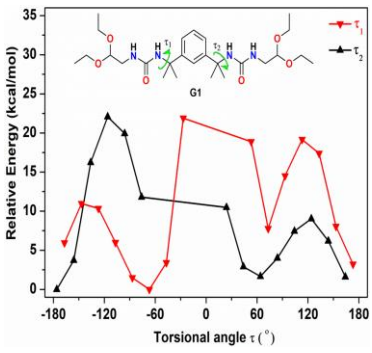

Figure 2.6 Relative energy profile diagram with respect to varied dihedral angle (τ_1 & τ_2) of **G1**

2.2.2 Polymorph Screening of G1:

Polymorph screening for **G1** was carry out using solution phase crystallization method in different solvents.

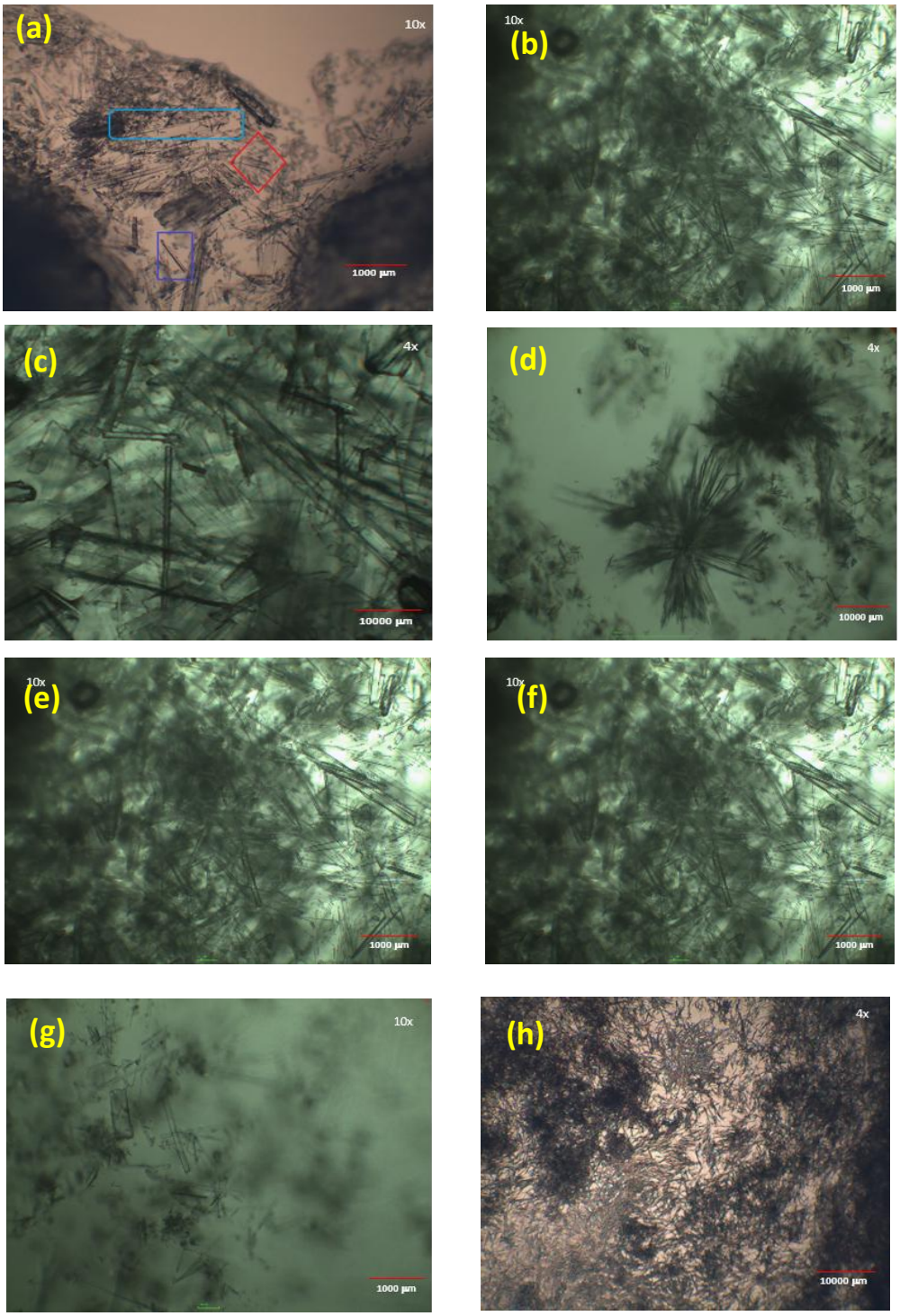

Figure 2.7 Microscopic images of **G1** crystallized from different solvents, (a) Ethanol, (b) DMF, (c) DMSO, (d) DMSO-H_2O, (e) MeOH, (f) Ethylene glycerol, (g) Glycerol, (h) Nitromethane

The outputs of polymorph screening experiment were analysed with powder XRD patterns and DSC endotherms. Three different types of PXRD patterns were observed (denoted as **G1** Form I, II, and III) and further analysis of these samples with DSC confirmedthat all three forms are distinct polymorphic phases of **G1** (shown in Figures 2.8 and 2.9a).

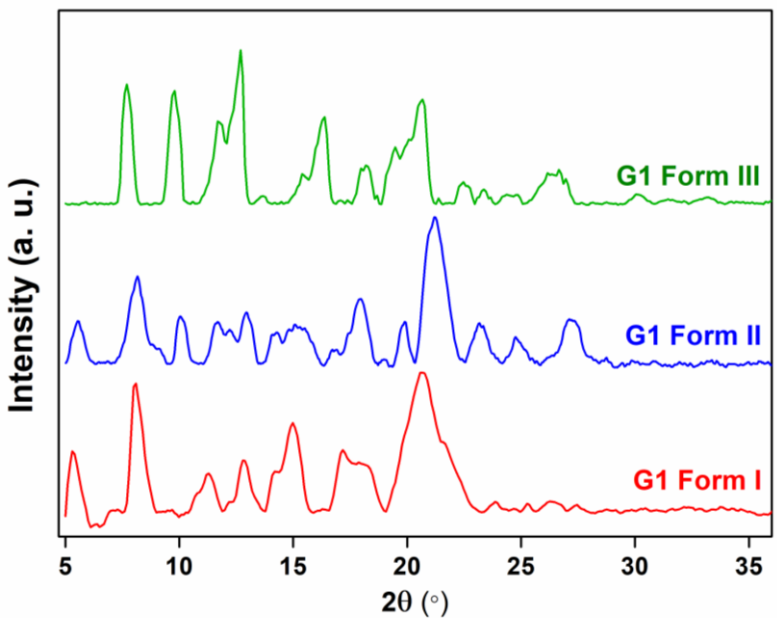

Figure 2.8 Overlay powder X-ray diffraction (PXRD) patterns of the three polymorphs of **G1**

FT-IR spectra of **G1** polymorphs were distinct and can be easily identified by N–H stretching frequency; 3344 cm^{-1}, 3337 cm^{-1},and 3359 cm^{-1} for **G1** Form I, II, and III respectively (Figure 2.9b). Shifting in N–H stretching frequency among the **G1** polymorphs arises due to different natures and strengths of H–bondings between the urea moieties. Solvent crystallization results are tabulated in Table 2.3 along with the nature of the solid phase (polymorphic form).

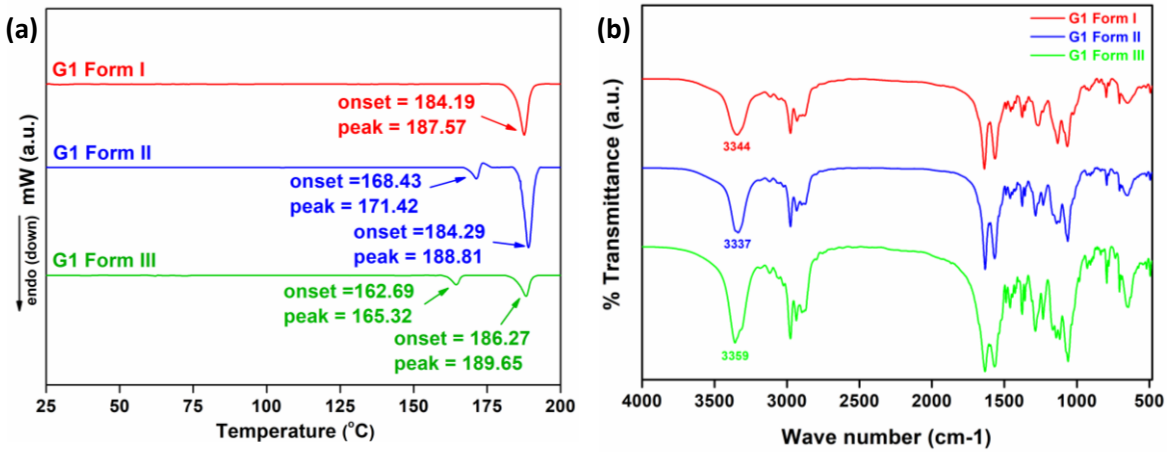

Figure 2.9 DSC endotherms (a) and FT-IR spectra (b) of the **G1** polymorphs

The DSC endotherms revealed **G1** Form II (onset 168.4 °C) and **G1** Form III (onset 162.7°C) were metastable forms and transformed into **G1** Form I (onset 184.1°C) (Figures 2.9a). The observed phase transformations were corroborated with heat-cool-heat cycle DSC experiments [44]. The disappearance of the endo peak at 168.4° C during reheating in DSC endotherm confirms the phase transition of **G1** Form II → Form I (Figure 2.10a). Correspondingly the disappearance of the endo peak at 162.7°C in the reheat cycle confirmed the phase transition of **G1** Form III → Form I (Figure 2.10b).

FT-IR spectra of polymorphs (**G1** Form II and III) were collected before and after heating where it was observed that the validation of phase transformations were in line with the DSC results (shown in Figures 2.10c and d).

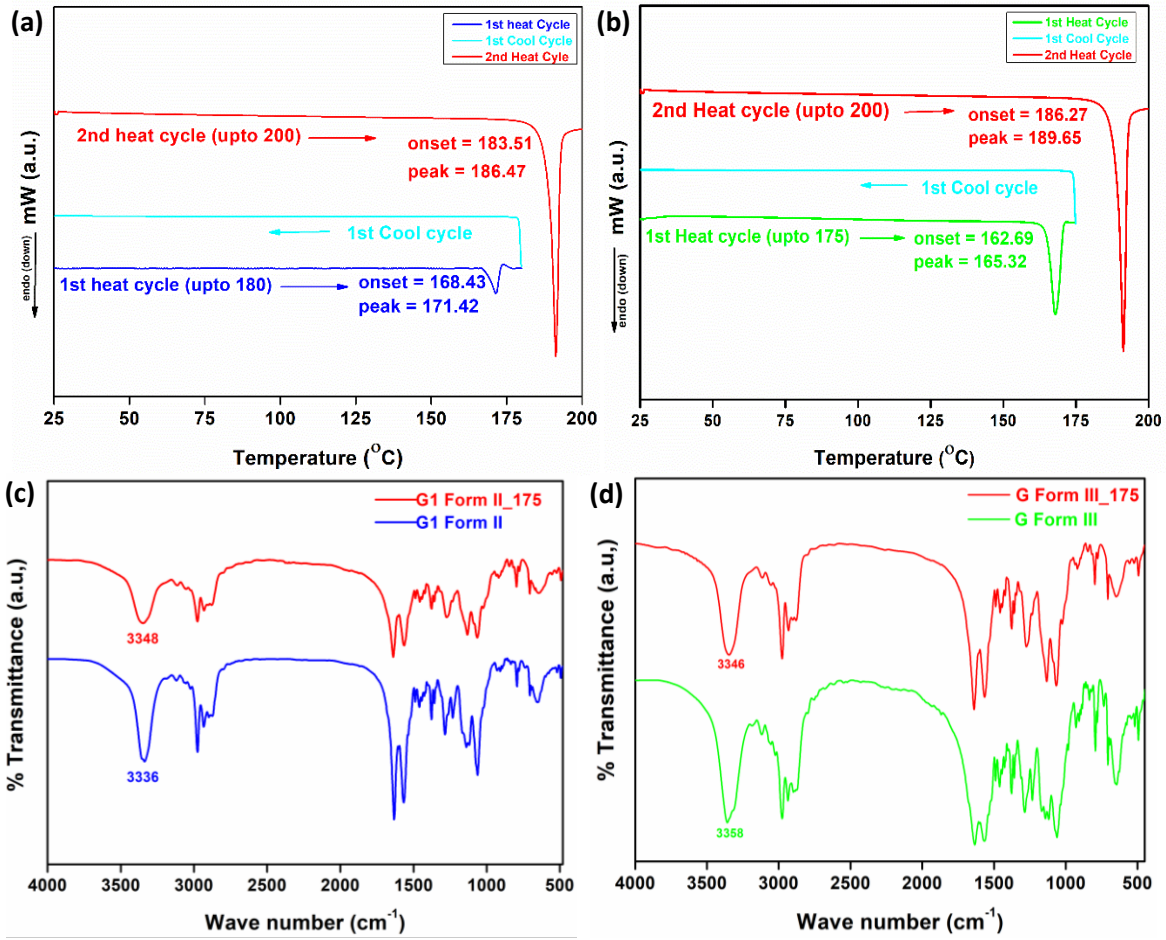

Figure 2.10 Transformation of polymorphs of **G1**: DSC heat-cool-heat cycle for **G1** Form II (a), and III (b); IR spectra of polymorph before and after phase transformation of **G1** Form II (c) and III (d)

A summary of phase changes that occurred between polymorphs as a function of temperature and solvent is depicted in the Figure 2.11.

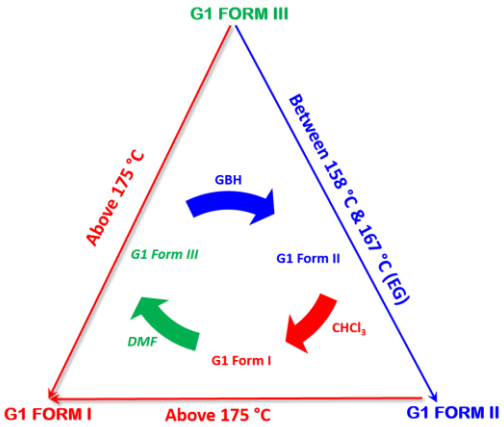

Figure 2.11 Graphical representation of phase transformations among the **G1** polymorphs

Table 2.3 Result of polymorph screening of **G1**using solution phase crystallization method

Sl.No	Solvent	Polymorph	Sl.No	Solvent	Polymorph
01	Methanol	**G1 Form III**	11	DMSO	**G1 Form III**
02	Ethanol	**G1 Form III**	12	DMSO-H_2O	**G1 Form III**
03	Propanol	**G1 Form III**	13	DMF	**G1 Form III**
04	2-Propanol	**G1 Form III**	14	THF	**G1 Form I**
05	Butanol	**G1 Form III**	15	1,4-Dioxane	**G1 Form I**
06	2-Butanol	**G1 Form III**	16	Chloroform	**G1 Form I**
07	t-Butanol	**G1 Form III**	17	GBH	**G1 Form II**
08	Glycerol	**G1 Form III**	18	Benzyl alcohol	**G1 Form III**
09	Ethylene glycol (EG)	**G1 Form III**	19	Ethyl acetate	**G1 Form I**
10	Ethylene glycol-H_2O	**G1 Form III**	20	Nitromethane	**G1 Form III**

*GBH = mixture of Glycerol:t-butanol-water in 2:1:3 ratio

To understand morphological differences among the polymorphs, images were recorded with the help of scanning electron microscopy (Figure 2.12). **G1** Form II and III show block-shaped morphologies whereas **G1** Form I was observed as lump/coagulation. However, the fine difference with the **G1** Form I of the molecule is marked from the images. Although morphologies of **G1** Form II and III are similar in shape but they are different in size distribution.

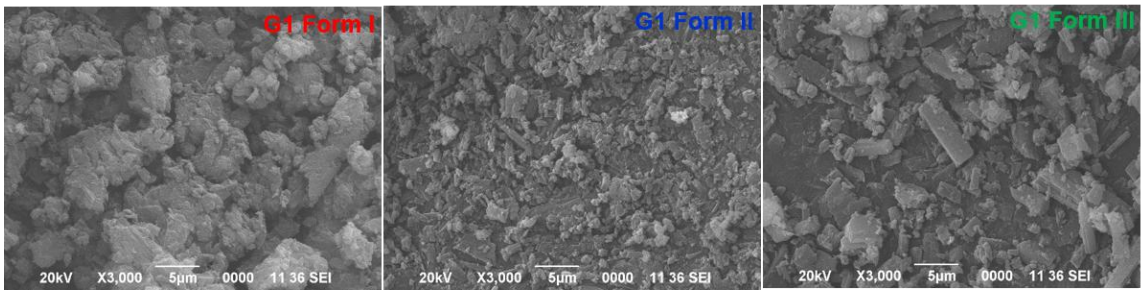

Figure 2.12 SEM images of all three polymorphs of **G1** isolated by solution recrystallization

As solubility plays a deciding role in the gelation process and polymorphs are known for their differences in solubility; we determined the solubility parameter of the **G1** polymorphs in toluene (toluene was chosen as it forms gel in many systems). Solubility were determined by solvent addition method which was further confirmed by thermogravimetric method (detailed experimental procedures were discussed in section 2.4.4) [46,47].

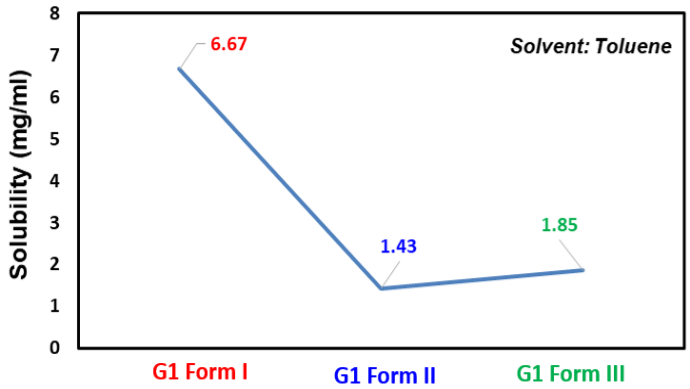

Figure 2.13 Graphical representation of solubility of the three polymorphs of **G1** in toluene at room temperature (25° C)

A clear difference in solubility among the polymorphs was observed and the solubility of **G1** Form I (6.67 mg/ml) is 3.6 and 4.6 times higher than **G1** Form II and III respectively (Figure 2.13).

The (i) conformational flexibility and concomitant nature of **G1**, and (ii) easy phase transformation between different phases became a serious hitch to nail down the gelation process demanding a strategic gel development process. Initially, the synthesized **G1** (i.e. **G1** Form I) was subjected to gel screening in toluene. The toluene was preferred to begin with the anticipation that it produce disarrays in the dangling hydrophobic precincts of **G1** by disrupting weak C–H···π and C–H···O interactions responsible for 3D packing in the solid form. Indeed it was a successful tryout that resulted in prophesied 1D taps propagating arbitrarily in the media. Finally, the 1D

hydrogen-bonded tapes entangled with each other in the presence of an external stimulus; thereby entrapping solvent molecules into the networks to form a gel (Figure 2.14).

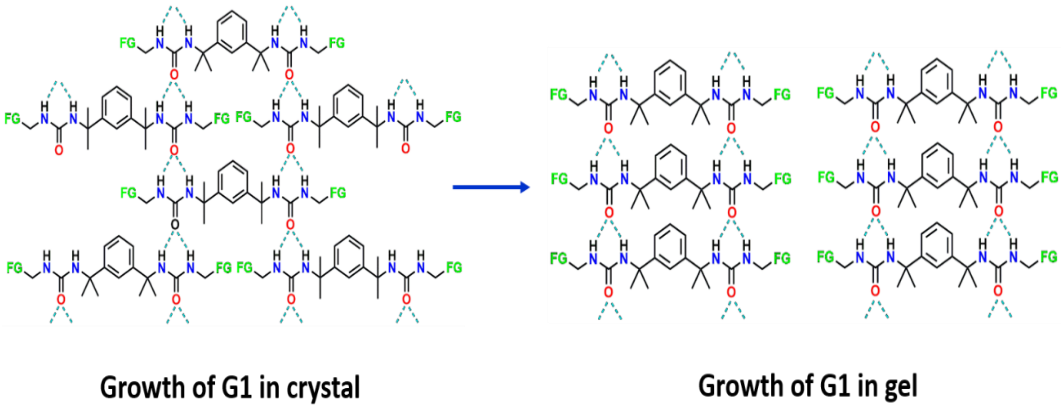

Figure2.14 Plausible molecular interactions between **G1** molecules in two different phases: crystalline state and the gel state. Solvent entrapment during self-assembly of gelator resulted gel instead of crystal. FG in the figure denotes a flexible group (diethyl acetal) attached to the core structure

Cooling down a hot gelator solution to room temperature without other disturbances is a common technique for gel evolution. However, during gel screening, sonication is used to homogenize the solution before/after applying trigger(s) for gelation. Interestingly, sonication itself triggered **G1** in the solution to transform into a gel. A similar observation was noted when a shaker was used for the same purpose. The response of **G1** in solution towards shaking (mechanical stimuli) intrigued us to examine mechanical grinding as a trigger for gelation. Grinding the mixture of **G1** and toluene in a mortar resulted in observe gelatinous precipitate within a few minutes. As a result, **G1** has turned out as multi stimuli responsive gelator (Figure 2.15).

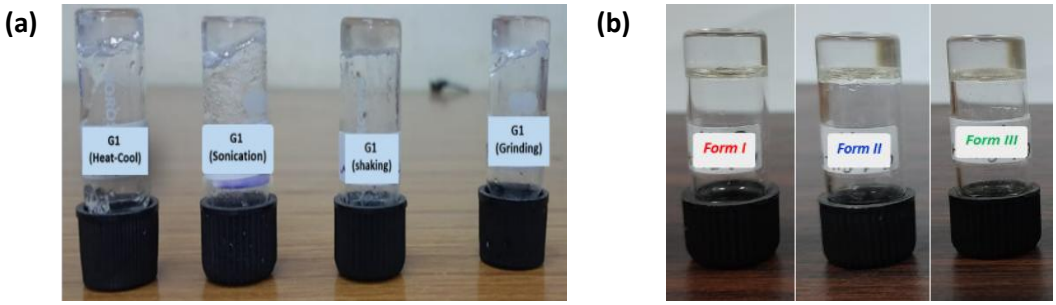

Figure 2.15 Pictures of the "vial inversion" test showing the gel formation in toluene: (a) **G1** Form I using different stimuli, (b) all three **G1** polymorphs using heat-cool stimuli

Stimuli responsiveness performance by the three polymorphic phases of **G1** towards gel evolution in different solvents was screened with those solvents that formed gel during heat-cool process (Tables 2.4 and 2.5). Screening results reflect heat-cool to

be the most effective stimulus that triggers all polymorphic phases into gel formation with at least 7 solvents. Unlike **G1** Form I, the other two forms failed to mark gel in the other three different stimuli (Figures 2.16). It is apparent that each polymorphic phase is controlled independently in the gelling solvents and does not respond the same way to each stimulus. It is also important to note that the phase behavior of **G1** polymorphs before and after gel evolution remained unaffected, supported by DSC and IR analysis (Figure 2.17).

Table 2.4 Gel screening for **G1** Form I in different solvents with 2 % (w/v)

Sl. No.	Name of Solvent	Remark	Sl. No.	Name of Solvent	Remark
1	Toluene	G	18	Pentanol	CS
2	o-Xylene	G	19	Water	P
3	m-Xylene	G	20	Acetic acid	CS
4	p-Xylene	G	21	DMF	CS
5	Ethyl acetate (EA)	G	22	DMSO	CS
6	Ethanol	CS	23	Acetonitrile	CS
7	Methanol	CS	24	Dioxane	CS
8	Propanol	CS	25	DCM	CS
9	2-Propanol	CS	26	1,2-DCE	G
10	Butanol	CS	27	Nitromethane (NM)	G
11	2-Butanol	CS	28	Nitrobenzene (NB)	G
12	t-Butanol	CS	29	Ethylene glycol (EG)	G
13	Tetrahydrofuran(THF)	CS	30	Mesitylene	G
14	Benzyl alcohol	CS	31	Glycerol	CS
15	Acetone	CS	32	Diethyl ether	P
16	Hexane	P	33	Di-isopropyl ether	P
17	Heptane	P	34	Cyclohexane	P

*Note: G = gel; CS = clear solution; P = precipitate.

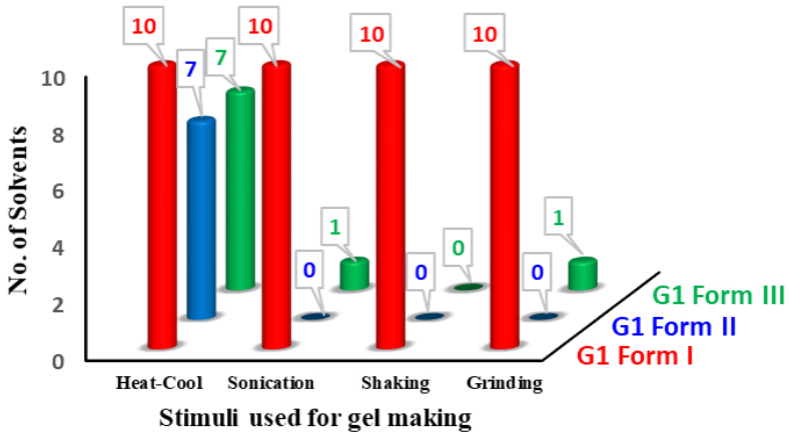

Figure 2.16 Graphical representation of gel formation of all the polymorphs against four different stimuli namely heat-cool, sonication, shaking and grinding

Table 2.5 Gel screening for all three polymorphs of **G1** using different procedures in gelling solvents using 2 % (w/v) gelator concentration

Procedure	G1 Form	T-X-M*	EA	NM	NB	1,2-DCE	EG
Heat-cool	I	**G**	**G**	**G**	**G**	**G**	**G**
	II	**PG**	P	CS	**G**	CS	F
	III	**WG**	P	P	**G**	P	**PG**
Sonication	I	**G**	S	**G**	**G**	CS	**PG**
	II	P	P	S	S	S	S
	III	P	P	P	P	CS	**PG**
Shaking	I	**G**	S	S	S	S	**PG**
	II	P	P	S	S	S	S
	III	P	P	S	S	S	S
Grinding	I	**G**	P	P	CS	P	**G**
	II	P	S	CS	CS	S	**PG**
	III	P	S	S	CS	P	**PG**

*Note: G = gel; P = precipitate; CS = clear solution; PG = partial gel; S = suspension; F= fibre; *T-X-M= Toluene, o-,m- & p-Xylene, Mesitylene.

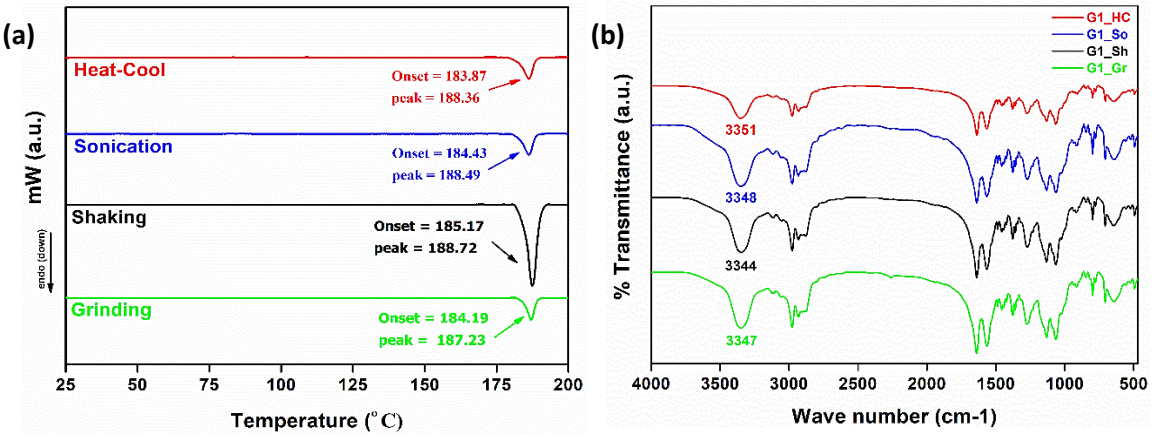

Figure 2.17 DSC endotherms (a) and IR (b) of toluene xerogels prepared by different stimuli using **G1** Form I showing phase behaviour of **G1** remained unaffected in the gel evolution process i.e. it remain in the **G1** Form I

Each stimulus used for triggering **G1** gel preparation may solubilize the gelator molecules to different extend (partly/completely soluble or smaller aggregates) and these lead to different fibrillary networks formation (pathway complexity). The role of stimuli on **G1** gels, considering toluene as the gelling solvent, and **G1** Form I (as it responded to all four stimuli) were investigated. The gel state was assessed based on four crucial parameters: T_{gel} (gel-sol transition temperature), M.G.C., rheological behavior (viscoelasticity), and gel fibre morphology. The T_{gel} was measured by the "ball-dropping" method for gel generated by exerting different stimuli at four different concentrations (ranging from 1 to 3 % w/v). From the T_{gel} vs. concentration graph (as shown in Figure 2.18a), it was observed that T_{gel} values of gels (from each stimulus) differing at all concentrations under consideration. T_{gel} indicates the thermal stability of a gel and above which due dissolution of the gel fibres 3D network of the gel breaks. These T_{gel} values can be correlated to the ability of the stimuli to dissolve the gelator (dissolved into molecules or aggregate state) in the solvent to initiate the gel formation. Another parameter to access a gelator is the M.G.C. value indicates the minimum concentration of a gelator to form a stable gel with the solvent considered and this value can fluctuate from solvent to solvent. The M.G.C. of **G1** Form I for each stimulus (checked by the 'vial inversion' test) was determined and values indicated that all stimuli required different amounts of gelator to form the gel (Figures 2.18b and 2.19).

The sonication and shaking require the lowest M.G.C. while heat-cool requires 0.8% (w/v) to form a stable gel. This can be understandable as shaking and sonication dispersed the gelators in solution in aggregated forms and as gelators were in an

aggregated state they assembled easily to gel fibres without leaving much gelator molecules in the solution. Contrastingly in the heat-cool process, the gelator solution was heated until clear a solution was observed (by the naked eye) and gelation was thought to be driven by supersaturation leaving some gelators in the solution (saturation point). This explains the high M.G.C value required for heat-cool stimuli gel. Thus, T_{gel} and M.G.C. parameters specify each stimulus can activate the gelator via dissimilar pathways to form a gel.

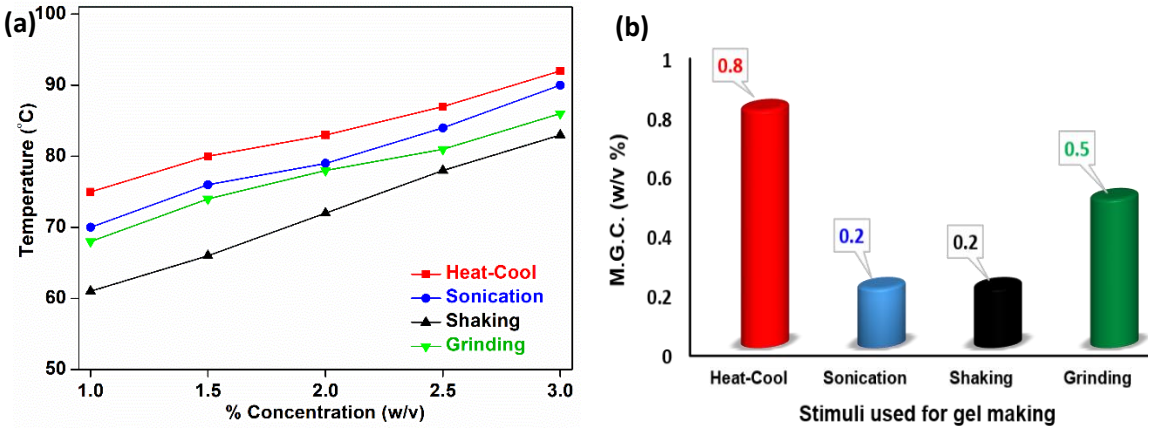

Figure 2.18 T_{gel} vs. gelator concentration (a) and M.G.C vs. Stimuli graphs of gels (of **G1** Form I in toluene) made from different stimuli: heat-cool (red), sonication (blue), shaking (black), and grinding (green) (b)

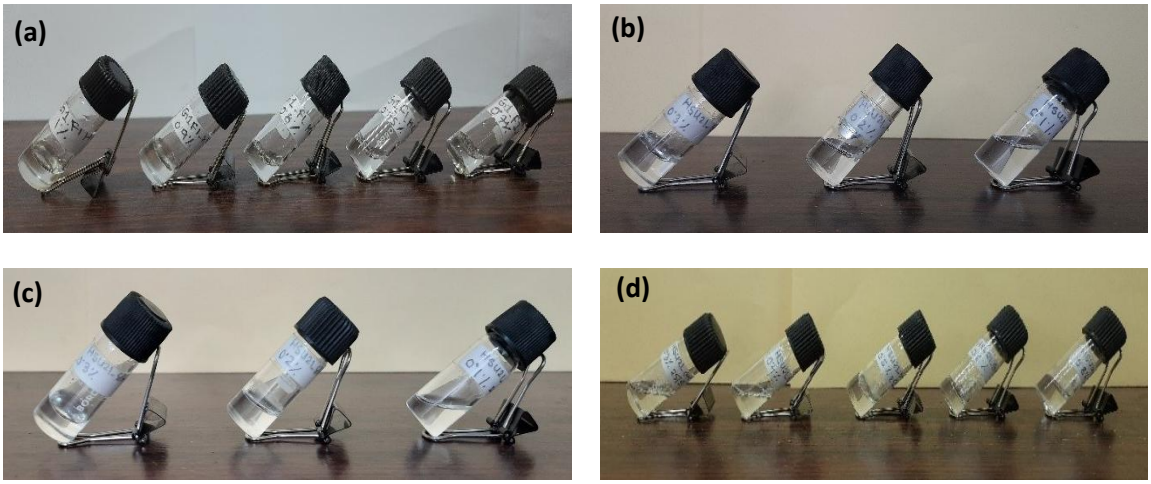

Figure 2.19 Pictures of "vial inversion" test during measuring M.G.C. of the **G1** Form I for gel preparation used all four stimuli. stimuli; (a) heat-cool, (b) sonication, (c) shaking, and (d) grinding

Rheological experiments were run to evaluate the viscoelastic nature of these gels. Two different methods, (i) strain (amplitude) sweep and (ii) frequency sweep were used to probe the gel state. At first, strain sweeps were performed to measure linear viscoelastic regions (LVR) and yield strain values which indicate the gel's viscoelastic

nature. Frequency sweep experiments were performed with the LVR region to check the stability of the gel state. From Figure 2.20a, strain sweep plots designate that gels made from the **G1** Form I followed by designated stimuli have different viscoelastic properties and behave differently with respect to applied strain. Rheological behaviours of the prepared gels are the outcome of the nature of the 3D fibre networks it formed in the gels. All four types of gels showed the gel-sol transition at strain value ranging from 3 to 8 % which indicated the supramolecular nature of the gels. From frequency sweep results it is evident that these gels are stable with respect to applied frequency (Figure 2.20b).

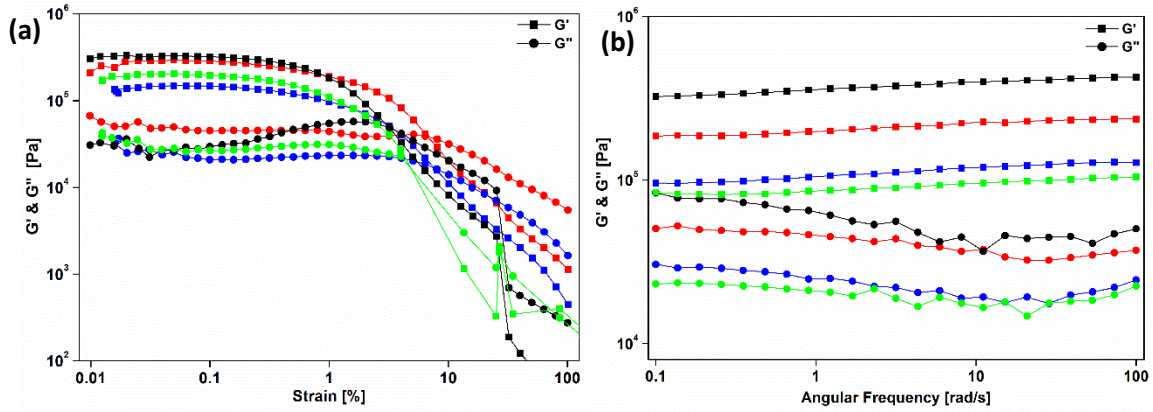

Figure 2.20 Amplitude sweep at constant frequency of 10 rad/s (a) and frequency sweep at a constant strain of 0.05 % strain within linear viscoelasticity region (LVR) (b) of **G1** Form I. Represented as storage modulus (G′), loss modulus (G″), heat-cool (red), sonication (blue), shaking (black), and grinding (green)

Rheological analysis confirms that gels prepared from each stimulus differ from each other. The morphology of gel fibres of the xerogels (different stimuli-induced gels) were examined using FESEM. Clear differences in fibre networks are observed from the recorded FESEM images. Gel made from heat-cool stimuli displayed a uniformly distributed thin fibrilar networkwhich entangled to form sample-spanning gel, whereas shaking-induced gel has a network of thick bundles of fibresthat breaks down easily during heating. This explains the difference in the T_{gel} values of heat-cool and shaking gel. However, a gel made from both sonication and grinding observeda combination of long thin fibers and thicker fiber bundles where long thin fibers was found to hold thicker fiber bundles to give well-connected gel fibre networks (Figure 2.21). Thus after evaluating all four crucial parameters of gels (T_{gel}, M.G.C., rheology and morphology), it is marked that each stimuli trigger the **G1** to form gels that are not identical. This is attributed to the aggregation of **G1** in distinctive manners induced by individual stimuli which also reflects the pathway complexity phenomenon in LMWG.

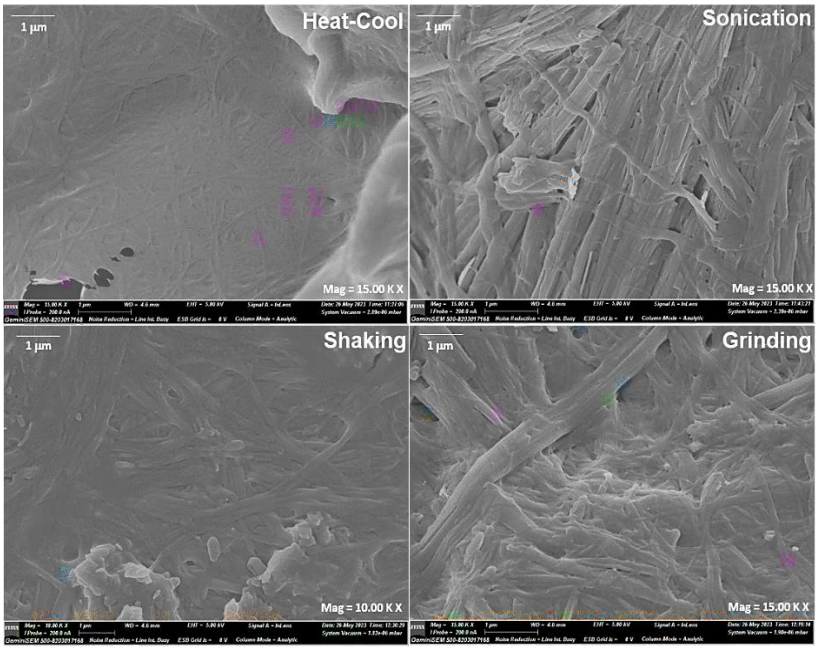

Figure 2.21 FESEM images (at magnification of 15K X except shaking which is at 10K X) of xerogels of **G1** Form I made from different stimuli heat-cool, Sonication, shaking, and grinding

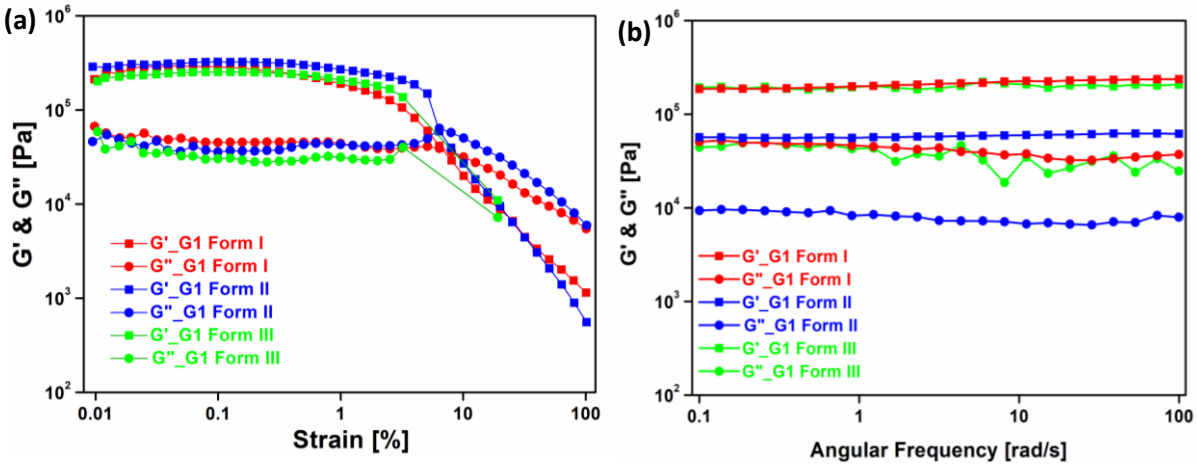

Figure 2.22 (a) Amplitude sweep at constant frequency of 10 rad/s and (b) frequency sweep at constant strain of 0.05 % under heat-cool stimuli for all three polymorphs of **G1**. G′ and G″ represent storage and loss modulus respectively

As mentioned above only polymorph **G1** FormI showed multi-stimuli responsiveness and the other forms failed to respond to stimuli except for heat-cool. Therefore, we started with evaluating the gels made by heat-cool stimuli using **G1** Form II and III to compare with **G1** Form I. The M.G.C. of these two polymorphs is found to be 3.8 % and 1 % respectively. Rheological analysis also supports better gelling performances of **G1** Form I than the other two polymorphs (Figure 2.22).

During the gel screening of **G1** Form II and III, it was observed that they precipitated out instead of forming gel under application of stimuli such as sonication, shaking, and grinding. We inspected some of the precipitates using electron microscopy. SEM images showed that they did not grow into fibril network and remained in their crystalline state (Figure 2.23).

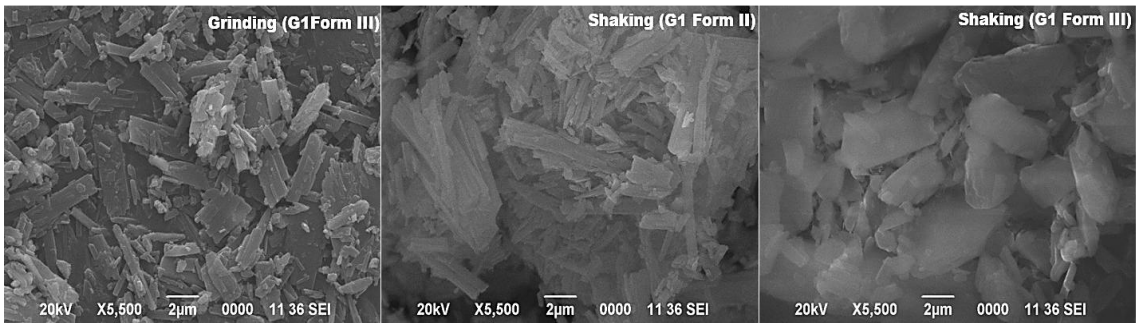

Figure 2.23 SEM images of precipitates of **G1** Form II and III obtained during gel screening using different stimuli

The early precipitation/crystallization of **G1** Form II and III rather than gel formation could be rationalized from their low solubility in the respective solvent. This 3 to 4 fold difference in solubility among the polymorphs is the key reason why only **G1** Form I responded to multiple stimuli in the gel evolution process. To make sure, we further increased the solubility of **G1** Form II and III by heating and obtaining a clear solution before it was subjected to other external stimuli. Interestingly, this time both the polymorphs responded to the stimuli to give gels (Figures 2.24 and 2.25).

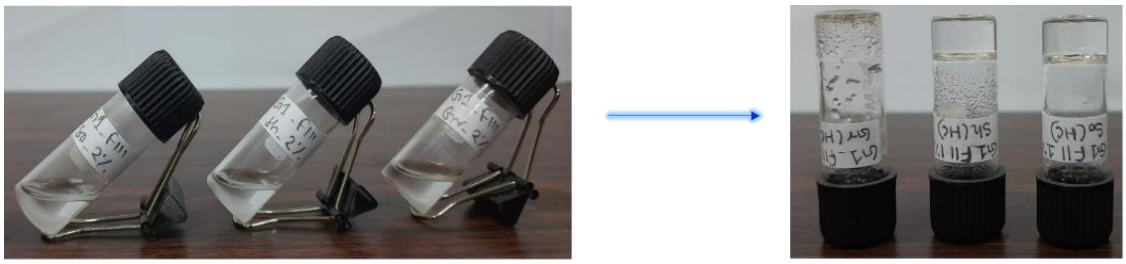

Figure 2.24 Pictures showing stimuli responsiveness of **G1** Form II after applying heating (Left: sonication, shaking and grinding; Right: grinding, shaking and sonication respectively)

Figure 2.25 Pictures showing stimuli responsiveness of **G1** Form III before applying heating (No Gel; from left: sonication, shaking and grinding); after applying heating (Gel formed; from right: grinding, shaking and sonication respectively)

2.3 SUMMARY

In this work, we have synthesized a bis-urea based gelator **G1** and isolated three polymorphic forms of it. All three polymorphs showed differences in their solubility parameter and **G1** Form I is more soluble than the other two forms. This difference in solubility played a crucial role in the stimuli responsiveness of the polymorphs. **G1** Form I which had better solubility responded to four stimuli (heat-cool, sonication, shaking and grinding), and on the other hand less soluble forms i.e. **G1** Form II and III only responded to heat-cool (considering toluene as a gelling solvent) only (Scheme 2.3).

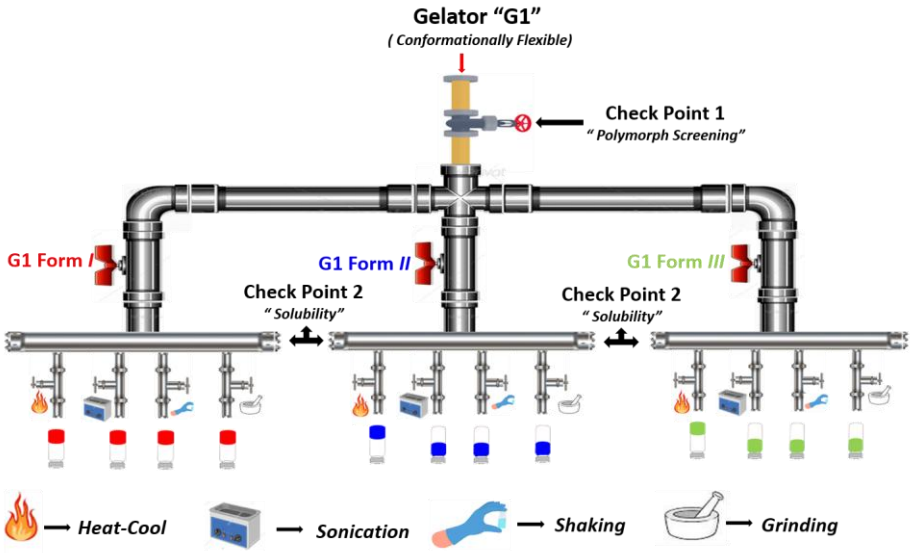

Scheme 2.3 Solid state polymorph screening of synthesized LMWG followed by gel screening leading to segregation of stimuli-responsive polymorphs yielding different gel performances in the prophecy of gel-sol transition temperature (T_{gel}), minimum gelator concentration (M.G.C.), morphology control, and allied rheological properties

Moreover, gels formed by different stimuli were found to have different properties (T_{gel}, M.G.C., gel fibre morphology, and allied rheological properties) and this

difference is thought to arise from the extent to which each stimulus solubilizes the gelator in the solvent. To tune such long-term stability of dispersion the solid state polymorphism behavior of the gelator is discovered as a critical phenomenon in deciding the performance of the gelator. It is so interesting that McCrone, specified that every compound has different polymorphic forms though the number of forms known for a given compound is proportional to the time and energy spent in research on that compound [48]. Rightly the impact of polymorphic forms on the drug development process is very resilient in the pharma R&D sectors manifested by numerous patent lawsuits. The gelation performance is first controlled by the weak non-covalent interactions, solubility, followed by self-assembly pathways in the gelling solvents before use of external stimuli. External stimuli such as heat-cool, sonication, shaking, and a fresh approach to mechanochemical grinding stated now can help in adopting different pathways in three-dimensional network formations resulting in different gels. Making different gels from a single relatively advantageous for their use in diverse applications. To obtain control over the crystallization event of drugs and the predicted gel systems will be a potential tool. Introducing flexible end groups into the main framework of a gelator is a well-known design strategy, but the risk of occurrence of different crystalline polymorphic phases by embracing conformational disparities leads to variation in the gelator's performance. This study thereby demonstrated the importance to identify different solid phases of a gelator molecule that will turn out to be a mandate to offer the way to evade glitches in the formation process of coveted gels.

2.4 EXPERIMENTAL SECTION

2.4.1 Materials:

All the chemicals used were brought from standard commercial sources and were used as such without further purification (exceptions were mentioned in the procedures). Aminoacetaldehyde diethyl acetal and 1,3-bis(2-isocyanto-2-propyl)benzene were purchased from TCI. All solvents used in experiments are of laboratory grade and purchased from SRL.

2.4.2 Instrumental Details:

FTIR data were recorded in the frequency range of 600−4000 cm^{-1}in Perkin Elmer SPECTRUM 100.Powder diffraction patterns were recorded on a BRUKER AXS diffractometer using Cu Kα radiation (λ= 1.54 Å), tube voltage of 40 kV, and 40 mA current. Intensities were measured from 5° to 50° 2θ with 0.01 rad.

Single crystal Xray diffractions were collected on a X-ray Diffractometer (Make: Bruker Model: D8 Quest) using Mo Kα (λ =0.71073 Å) radiation. The structure was solved and refined using SHELXL.NMR spectra were recorded using a 400 MHz Bruker NMR Make: Bruker Model: AVANCE (^{1}H: 400 MHz; ^{13}C: 100 MHz) spectrometer at room temperature using deuterated solvent $CDCl_3$. HRMS (Xevo G2-XS QT of (Waters) mass spectrometer using electron spray ionization mass). Elemental analysis was performed by using a PERKIN ELMER, USA, 2400 SERIES 2.

Both TGA and DSC data were collected in SHIMADZU model TGA-50 and DSC-60; respectively and analysed using Software: TA-60WS. Heat-cool-heat experiments were recorded in DSC Analyzer of Make: Mettler Toledo / TA Instruments.

Rheological experiments were performed using a Modular Compact Rheometer (MCR72) of Anton Paar, Austria and analysed using Anton Paar RheoCompass™ V1.20.471. Measuring system of Parallel plate (25mm Plate diameter, 1 mm measuring gap) at 25 °C used to perform the experiments. Samples of the gels were prepared in general at 2 (w/v) % (of 2ml volume) in 5mL glass vials. The obtained gels were transferred on to the centre of the plate of the rheometer using a spatula. The oscillation sweep measurements were performed to estimate linear viscoelastic region (LVR) (with constant frequency of 10 rad/s) for the prepared gels and frequency sweep measurements were performed to check stability of the gels with respect to frequency range of 0.1 to 100 rad/s (at constant 0.01 % strain, within the range of LVR).

Gel samples were air dired to transform into xero gels and then xerogels were use to get electron microscopy images for both SEM and FESEM technique. SEM Images were recorded on JEOL model JSM 6390LV scanning electron microscope. FESEM images were recorded in Gemini 500 FE-SEM. Samples were coated with 2 nm of Pt before recording in both instruments.Microscopic images are recorded in Motic Microscope 3.O^{+} and analysized with Motic software.

2.4.3 Synthetic procedure and Characterization of G1:

2 mmol (0.29 ml) of aminoacetaldehyde diethyl acetal (ADA) in 20 ml dry chloroform was added dropwise to the 30 ml of dry chloroform solution of 1 mmol (0.23 ml) of 1,3-bis(2-isocyanto-2-propyl)benzene (ISB) and kept stirring for 12 h at room temperature. The reaction progress was monitored through TLC. The reaction mixture was evaporated to dryness. Recovered crude product was washed with water and air dried to get white powder. Obtained yield was 91% (0.46 g).

^{1}H NMR ($CDCl_3$, 400 MHz) δ (ppm) : 7.56 (s, 1H), 7.31 (s, 3H), 5.07 (s, 2H), 4.56 (t, 2H , *J*= 5.2 Hz) , 4.41 (t, 2H, *J*= 7 Hz), 3.63–3.42 (m, 8H), 3.22 (m, 4H,), 1.63 (s, 12H), 1.16 (t, 12H, *J*= 7.1). $^{13}C\{^{1}H\}$ NMR ($CDCl_3$, 101 MHz) δ (ppm) : 15.3, 30.2, 42.6, 55.2, 62.5, 101.4, 122.3, 123.7, 128.9, 147.3, 157.6. HRMS (ESI-TOF) m/z: $[M+H]^+$ calcd for $C_{26}H_{47}N_4O_6$ is 511.3496; found 511.3489. CHN analysis: calcd. C (61.15%), H (9.08%), N (10.97%); Found: C (60.78%), H (9.12%), N (10.62%).

2.4.4 Computational Details:

In order to check the energy variation in **G1** as a function of torsional angles (**τ_1** and **τ_2**), DFT calculations were performed using the functional B3LYP in conjunction with basis set 6-311G^{++} (d,p). All calculations have been done at GAUSSIAN 16 package. It is to be noted that the coordinates for **G1** Form III has been obtained from the CIF file (CCDC No. 2304758).

2.4.5 Polymorph screening:

G1 Form I was obtained directly from synthesis of **G1** and also obtained by recrystallization of other forms from 1,4-dioxane and THF. **G1** Form II was obtained by recrystallization of **G1** Form I in the mixture of glycerol/ t-butanol/water (GBH) in the ration 2:1:3. **G1** Form III was obtained by recrystallization of **G1** Form I in DMF.

2.4.6 Solubility measurement of G1:

Solubility measurement of the **G1** polymorphs using UV-Vis spectrometry was not possible to perform as **G1** don't have any observable peak (suitable for experimental consideration) in the range 200-800 nm. So we proceed with other available methods for solubilty measurement methods described below.

(i) Method I (Solvent addition method)

Solubility of the polymorphs were measured by adding solvent in small portion to a definite amount (here 10mg) of the polymorph and observed by eye whether a clear solution was obtain or not. If the polymorph remain undissolved, solvent added in small volume (50 μl) and continued the process till a clear solution was observed. Volume of solvent corresponding the clear solution was considered as amount of solvent required for dissolving 10mg of the polymorph at room temperature. Experiments were repeated three times and average of the values taken as the solubility parameter for the polymorph under consideration.

(ii) Method II (Thermogravimetric method):

Solubility of polymorphs of **G1** measured by the above method were verified by this method. Here solubility measurement of the polymorphs in toluene were conducted using a thermogravimetric method. For each polymorph, slurry was prepared by adding excess of the polymorph to 15 mL of toluene in glass vial (size = 30ml). The vials were kept at room temperature for a minimum of 48 h to allow the sample to reach equilibrium. Syringes were used to take a 7 mL aliquot of each solution separately. The extracted solutions were filtered through a 0.22 μm syringe filter and weighed in a Petri dish. The Petri dishes were left at room temperature for the solvent to evaporate and were weighed daily until a constant mass was achieved [46, 47].

2.4.7 Procedures for gel preparation:

Glass vial size: 5 ml; Solvent purity: Reagent grade; Concentration: % of w/v. Time required to form gel reduces with increase in the gelator concentration. Gelation at M.G.C. required time to form a stable gel. At M.G.C., sonication and shaking formed the gel fastest.

I. Heat-Cool process:

Required amount of **G1** and solvent (e.g. Toluene) were mixed in a glass vial and close the cap tightly. The glass vial was then heated on a hot plate till a clear solution was observed. The clear solution containing **G1** was kept undisturbed and allowed to cool down to room temperature. During the cooling process gel formation started.

II. Sonication process:

Required concentration of the mixture of **G1** and solvent was made in a glass vial. After closing the cap of the vial, vial was subjected to sonication (using Ultrasonicator bath) for 10 minutes to obtain a homogenous mixture. Then the vial was kept undisturbed and allowed the solution to form gel.

III. Shaking process:

Required concentration of the mixture of **G1** and solvent was made in a glass vial. After closing the cap of the vial, vial was subjected to shaking using vortex (shaker, make: IKA) for 10 minutes to obtain a homogenous mixture. Then the vial was kept undisturbed and allowed the solution to form gel. Shaking of the mixture can be performed by using hands.

IV. Grinding process:

In this process, required amount of **G1** taken in a mortar, solvent was then added and then grounded using the pestle for 5 minutes until the mixture turned into a viscous solution. Then this viscous solution transferred into the vial and kept undisturbed to allow the viscous solution to form gel.

2.4.8 Determination of Tgel and M.G.C. of gels:

I) T_{gel} measurement:

T_{gel} of gels with different concentrations are determined by 'ball drop' method. A small steel ball (0.118g, d ≈ 2 mm) was place on the top of the gel prepared (2ml) in a glass vial (5ml size) and the vial placed in an oil bath whose temperature increase at 1°C per minute. As the temperature increases, ball slowly went inside into the gel and the temperature at which the ball touches the bottom of the vial was recorded as T_{gel} of the gel. Measurements were repeated thrice for accuracy and average value of them was taken as the final value of T_{gel}.

II) M.G.C. measurement:

For measuring M.G.C., at first initial screening was done at 0.5, 1 and 2 % w/v; then screening process was narrow down to lower concentration range. Then M.G.C. was evaluated by checking the minimum concentration below which it failed to form gel and that minimum concentration was essential to form the gel was recorded as the M.G.C. value.

2.4.9 Gel screening:

a) Initial screening of solvents using G1 Form I :

Initial screening was done by adding 20 mg/ml of **G1** Form I in respective solvent and heated till clear solution obtained and kept undisturbed to cooling down to room temperature.

b) Gel screening by using different stimuli (heat-Cool, sonication, shaking and grinding):

Above mention procedures for gel preparation were used for the screening.

c) Gel screening for all three polymorphs (G1 Form I to III) using all four stimuli:

Above mention procedures for gel preparation using different stimuli were applied for gel screening.

2.5 REFERENCES

[1] Foster, J. A., Piepenbrock, M. O. M., Lloyd, G. O., Clarke, N., Howard, J. A., Steed, J. W. Anion-Switchable Supramolecular Gels for Controlling Pharmaceutical Crystal Growth. *Nature Chemistry*, 2:1037-1043, 2010.

[2] Saikia, B., Mulvee, M. T., Torres-Moya, I., Sarma, B., Steed, J. W. Drug Mimetic Organogelators for the Control of Concomitant Crystallization of Barbital and Thalidomide. *Crystal Growth & Design*, 20:7989-7996, 2020.

[3] Sharma, H., Kalita, B. K., Pathak, D., Sarma, B.Low Molecular Weight Supramolecular Gels as a CrystallizationMatrix. *Crystal Growth & Design*,24:17-37, 2023.

[4] (a) Roy, R.,Majumder, J., Datta, H. K., Parveen, R., Dastidar, P. Supramolecular Hydrogels Developed from Mafenide and Indomethacin as a Plausible Multidrug Self-Delivery System as Antibacterial and Anti-inflammatory Topical Gels. *ACS Applied Bio Materials*, 5:610-621, 2022. (b) El-QarraL, H., Cosottini, N., Tangsombun, C., Smith, D. K. Formulation and Release of Active Pharmaceutical Ingredients using a Supramolecular Self-healing Two-component Gel. *Chemistry—A European Journal*, p.e202402530, 2024.

[5] Babu, S. S., Prasanthkumar, S., Ajayaghosh, A. Self-Assembled Gelators for Organic Electronics. *Angewandte Chemie International Edition*, 51:1766– 1776, 2012.

[6] (a) Rodríguez-Llansola, F., Miravet, J. F., Escuder, B.A Supramolecular Hydrogel as a Reusable Heterogeneous Catalyst for the Direct Aldol Reaction. *Chemical Communications*,47:7303-7305, 2009. b) Escuder, B., Rodríguez-Llansola, F., Miravet, J. F. Supramolecular Gels as Active Media for Organic Reactions and Catalysis. *New Journal of Chemistry*, 34:1044-1054, 2010. (c) Slavík, P.,Trowse, B. R., O'Brien, P.,Smith, D. K. Organogel Delivery Vehicles for the Stabilization of Organolithium Reagents. *Nature Chemistry*, 15:319-325, 2023.

[7] Vibhute, A. M., Sureshan, K. M. How Far are We in Combating Marine Oil Spills by Using Phase-Selective Organogelators? *ChemSusChem*, 13:5343-5360, 2020.

[8] a) Dastidar, P. Supramolecular gelling agents: can they be designed? *Chemical Society Reviews*, 37:2699-2715, 2008. b) Adarsh, N. N., Sahoo, P., Dastidar, P. Is a Crystal Engineering Approach useful in Designing Metallogels? A Case Study. *Crystal Growth& Design*, 10:4976-4986, 2010. c) Dastidar, P. Designing Supramolecular Gelators: Challenges, Frustrations, and Hopes. *Gels*, 5:15, 2019.

[9] Bera, S. S., Basu, S., Jana, B., Dastidar, P. Real-time Observation of Macroscopic Helical Morphologies under Optical Microscope: A Curious Case of π–π Stacking Driven Molecular Self-assembly of an Organic Gelator Devoid of Hydrogen Bonding. *Angewandte Chemie International Edition*, 62:e202216447, 2022.

[10] Terech, P., Weiss, R. G. Low Molecular Mass Gelators of Organic Liquids and the Properties of Their Gels. *Chemical Reviews*, 97:3133-3160, 1997.

[11] Weiss, R. G. The Past, Present, and Future of Molecular Gels. What is the Status of the Field, and Where is It Going? *Journal of the American Chemical Society*, 136:7519-7530, 2014.

[12] Colquhoun, C., Draper, E. R., Schweins, R., Marcello, M., Vadukul, D., Serpell, L. C., Adams, D. J. Controlling the Network Type in Self-Assembled Dipeptide Hydrogels. *Soft Matter*, 13:1914-1919, 2017.

[13] Gao, J.,Wu, S., Rogers, M. A. Harnessing Hansen Solubility Parameters to Predict Organogel Formation. *Journal of Materials Chemistry*, 22:12651-12658, 2012.

[14] Minami, K., Mizuta, M.,Suzuki, M.,Aizawa, T., Arai, K. Determination of Kamlet–Taft Solvent Parameters Π* of High Pressure and Supercritical Water by the UV-Vis Absorption Spectral Shift of 4-Nitroanisole. *Physical Chemistry Chemical Physics*, 8, 2257-2264, 2006.

[15] Potter, C. B., Davis, M. T., Albadarin, A. B., Walker, G. M. Investigation of the Dependence of the Flory–Huggins Interaction Parameter on Temperature and Composition in a Drug–Polymer System. *MolecularPharmaceutics*,15:5327-5335, 2018.

[16] Diehn, K. K., Oh, H., Hashemipour, R., Weiss, R. G., Raghavan, S. R. Insights into Organogelation and Its Kinetics from Hansen Solubility Parameters. Toward a Priori Predictions of Molecular Gelation. *Soft Matter,*10:2632-2640, 2014.

[17] Babu, S. S., Mahesh, S., Kartha, K. K., Ajayaghosh, A.Solvent-Directed Self-Assembly of π Gelators to Hierarchical Macroporous Structures and Aligned Fiber Bundles. *Chemistry—An Asian Journal*, 4:824-829, 2009.

[18] Wang, Y., de Kruijff, R. M., Lovrak, M., Guo, X., Eelkema, R., van Esch, J. H. Access to Metastable Gel States Using Seeded Self-Assembly of Low-Molecular-Weight Gelators. *Angewandte Chemie International Edition*, 58, 3800-3803, 2019.

[19] Draper, E. R., Adams, D. J. Controlling Supramolecular Gels. *Nature Materials*, 23:13-15, 2024.

[20] Yamanaka, M., Fujii, H.Chloroalkane Gel Formations by Tris-Urea Low Molecular Weight Gelator Under Various Conditions. *Journal of Organic Chemistry*, 74:5390-5394, 2009.

[21] Pramanik, A., Karimadom, B. R., Kornweitz, H., Levine, M.Sonication-Induced, Solvent-Selective Gelation of a 1, 8-Napthalimide-Conjugated Amide: Structural Insights and Pollutant Removal Applications. *ACS Omega*, 6:32722-32729, 2021.

[22] Naota, T., Koori, H. Molecules That Assemble By Sound: An Application to the Instant Gelation of Stable Organic Fluids. *Journal of the American Chemical Society*, 127: 9324-9325, 2005.

[23] Yamanaka, M. Nakamura, T., Nakagawa, T.,Itagaki, H. Reversible Sol–Gel Transition of a Tris–Urea Gelator that Responds to Chemical Stimuli. *Tetrahedron Letters*, 48:8990-8993, 2007.

[24] Piepenbrock, M. O. M., Clarke, N., Steed, J. W. Shear Induced Gelation in a Copper (II) Metallogel: New Aspects of Ion-Tunable Rheology and Gel-Reformation by External Chemical Stimuli. *Soft Matter,* 6:3541-3547, 2010.

[25] Frkanec, L., Jokić, M., Makarević, J., Wolsperger, K., Žinić, M. Bis (Pheoh) Maleic Acid Amide−Fumaric Acid Amide Photoizomerization Induces Microsphere-to-Gel Fiber Morphological Transition: the Photoinduced Gelation System. *Journal of the American Chemical Society*, 124:9716-9717, 2002.

[26] Tsuchiya, K., Orihara, Y., Kondo, Y., Yoshino, N., Ohkubo, T., Sakai, H.,Abe, M. Control of Viscoelasticity Using Redox Reaction. *Journal of the American Chemical Society*, 126:12282-12283, 2004.

[27] Colquhoun, C., Draper, E. R., Schweins, R., Marcello, M., Vadukul, D., Serpell, L. C., Adams, D. J. Controlling the Network Type in Self-Assembled Dipeptide Hydrogels. *Soft Matter*, 13:1914-1919, 2017.

[28] Abraham, B. L., Agredo, P., Mensah, S. G., Nilsson, B. L. Anion Effects on the Supramolecular Self-Assembly of Cationic Phenylalanine Derivatives. *Langmuir*, 38:15494-15505, 2022.

[29] Maeda, H.Anion-Responsive Supramolecular Gels. *Chemistry—A European Journal*, 14:11274-11282, 2008.

[30] Cardoso, A. Z., Mears, L. L. E., Cattoz, B. N., Griffiths, P. C., Schweins, R., Adams, D. J. Linking Micellar Structures to Hydrogelation for Salt-Triggered Dipeptide Gelators. *Soft Matter*, 12:3612-3621, 2016.

[31] Chen, L., Revel, S., Morris, K. C., Serpell, L., Adams, D. J. Effect of Molecular Structure on the Properties of Naphthalene− Dipeptide Hydrogelators. *Langmuir*, 26:13466-13471, 2010.

[32] Contreras-Montoya, R., Smith, J. P., Boothroyd, S. C., Aguilar, J. A., Mirzamani, M., Screen, M. A., Yufit, D. S., Robertson, M., He, L., Qian, S., Kumari, H., Steed, J. W. Pathway Complexity in Fibre Assembly: From Liquid Crystals to Hyper- Helical Gelmorphs. *Chemical Science*, 14:11389-11401, 2023.

[33] Foster, J. S., Żurek, J. M., MS Almeida, N., Hendriksen, W. E., le Sage, V. A. A., Lakshminarayanan, V., Thompson, A. L., Banerjee, R., Eelkema, R., Mulvana, H., Paterson, M. J., van Esch, J. H., Lloyd, G. O. Gelation Landscape Engineering Using a Multi-Reaction Supramolecular Hydrogelator System. *Journal of the American Chemical Society*, 137, 14236-14239, 2015.

[34] Schwaller, D., Yilmazer, S., Carvalho, A.,Collin, D., Mésini, P. J.Impact of Polymorphism in Oleogels of N-Palmitoyl-L-Phenylalanine. *SoftMatter*, 19:4277-4285, 2023.

[35] Ostuni, E. Kamaras, P., Weiss, R. G.Novel X-Ray Method for in-situ Determination of Gelator Strand Structure: Polymorphism of Cholesteryl Anthraquinone-2-Carboxylate. *Angewandte Chemie International Edition*, 35:1324-1326, 1996.

[36] van der Laan, S., Feringa, B. L., Kellogg, R. M., van Esch, J. Remarkable Polymorphism in Gels of New Azobenzene Bis-Urea Gelators. *Langmuir*, 18: 7136-7140, 2002.

[37] Rodríguez-Llansola, F., Miravet, J. F., Escuder, B. A Supramolecular Hydrogel as a Reusable Heterogeneous Catalyst for the Direct Aldol Reaction. *Chemical Communications*,47:7303-7305, 2009.

[38] Díaz-Oltra, S., Berdugo, C., Miravet, J. F., Escuder, B. Study of the Effect of Polymorphism on The Self-Assembly and Catalytic Performance of an L-Proline Based Molecular Hydrogelator. *New Journal of Chemistry*, 39:3785-3791, 2015.

[39] Chemburkar, S. R.,Bauer, J., Deming, K., Spiwek, H., Patel, K., Morris, J., Henry, J., Spanton, S., Dziki, W., Porter, W., Quick, J., Bauer, P., Donaubauer, J., Narayanan, B. A., Soldani, M., Riley, D., McFarland, K. Dealing with the Impact

of Ritonavir Polymorphs on the Late Stages of Bulk Drug Process Development *Organic Process Research & Development*, 4:413-417, 2000.

[40] Bora, P., Saikia, B., Sarma, B. Oriented Crystallization on Organic Monolayers to Control Concomitant Polymorphism. *Chemistry—A European Journal*, 26:699-710, 2020.

[41] Chen, J., Sarma, B., Evans, J. M., Myerson, A. S. Pharmaceutical Crystallization. *Crystal Growth & Design*, 11:887-895, 2011.

[42] Khatioda, R., Saikia, B., Das, P. J., Sarma, B. Solubility and In Vitro Drug Permeation Behavior of Ethenzamide Cocrystals Regulated in Physiological pH Environments. CrystEngComm, 19:6992-7000, 2017.

[43] Yang, X., Sarma, B., Myerson, A. S. Polymorph Control of Micro/Nano-Sized Mefenamic Acid Crystals on Patterned Self-Assembled Monolayer Islands. *Crystal Growth & Design*, 12:5521-5528, 2012.

[44] Sarma, B., Roy, S., Nangia, A. Polymorphs of 1, 1-Bis (4-Hydroxyphenyl) Cyclohexane and Multiple Z′ Crystal Structures by Melt and Sublimation Crystallization. Chemical Communications, 47:4918-4920, 2006.

[45] Gaussian 16, Revision C.01, Frisch, M. J.,Trucks, G. W., Schlegel,H. B.,Scuseria, G. E.,Robb, M. A.,Cheeseman, J. R., Scalmani, G.,Barone, V., Petersson, G. A., Nakatsuji, H., Li, X., Caricato,M., Marenich, A. V.,Bloino, J., Janesko, B. G., Gomperts, R., Mennucci, B., Hratchian, H. P., Ortiz, J. V., Izmaylov, A. F., Sonnenberg, J. L., Williams-Young, D., Ding, F., Lipparini, F., Egidi, F., Goings, J., Peng, B., Petrone, A., Henderson, T,. Ranasinghe, D., Zakrzewski, V. G., Gao, J., Rega, N., Zheng, G., Liang, W., Hada, M., Ehara, M.,Toyota, K., Fukuda, R., Hasegawa, J., Ishida, M., Nakajima, T.,Honda, Y., Kitao, O., Nakai, H., Vreven, T., Throssell, K., Montgomery, J. A. Jr., Peralta, J. E., Ogliaro, F., Bearpark, M. J.,Heyd, J. J., Brothers, E. N., Kudin, K. N., taroverov, V. N., Keith, T. A., Kobayashi, R., Normand, J., Raghavachari, K., Rendell, A. P., Burant, J. C., Iyengar, S. S., Tomasi, J., Cossi, M., Millam, J. M., Klene, M., Adamo, C., Cammi, R.,Ochterski, J. W., Martin, R. L., Morokuma, K., Farkas, O., Foresman, J. B., Fox, D. J.Gaussian, Inc., Wallingford CT, 2016.

[46] Preston, J. A., Parisi, E., Murray, B., Tyler, A. I., Simone, E.Elucidating the Polymorphism of Xanthone: A Crystallization and Characterization Study. *Crystal Growth & Design*, 24(8):3256-3268, 2024.

[47] Wang, Y., Lin, K., Jia, W., Yu, Q. Measurement and Correlation of Solubility of l-Valine, l-Isoleucine, l-Methionine, and l-Threonine in Water + tert-Butanol from 283.15 to 328.15 K. *Journal of Chemical & Engineering Data*,66(1):677- 683, 2020.

[48] McCrone, W. C. Polymorphism in Physics and Chemistry of the Organic Solid State, Vol II (Eds.: D. Fox, M. M. Labes and A. Weissenberg), Interscience, New York, 1965, pp.726

[49] Bruker, A.; Saint, AXS Inc.,: Madison, W. Inc. 2008, 64, 112.

[50] SAINT Plus (v 6.14); Bruker, A.; Saint, AXSInc.,: Madison, W. Inc., Madison, WI,. 2008, 64, 112.

[51] Spek, A. L. PLATON, Utrecht University, The Netherlands; b) AL Spek. J. Appl. Crystallogr 2003, 36 (7).

[52] Barbour, L. J. X-Seed, Graphical Interface to SHELX-97 and POV-Ray. Univ. MissouriColumbia, Columbia, MO 1999.